Journal of the Korean Society for Nondestructive Testing
Vol. 28, No. 6 (2008. 12)

Influence of Dislocation Substructure on Ultrasonic Velocity under Tensile Deformation

C. S. Kim*, Cliff J. Lissenden*, Kae-Myhung Kang** and Ik-Keun Park***†

Abstract The influence of dislocation substructure of metallic materials on ultrasonic velocity has been experimentally investigated. The test materials of pure Cu, brass (Cu-35Zn), 2.25Cr-1Mo steel, and AISI 316 with different stacking fault energy (SFE) are plastically deformed in order to generate dislocation substructures. The longitudinal wave velocit (C_L) decreases as a function of tensile strain in each material. The C_L of Cu-35Zn and AISI 316 decreases monotonously with tensile strain, but C_L of Cu and 2.25Cr-1Mo steel shows plateau phenomena due to the stable dislocation substructure. The variation of ultrasonic velocity with the extent of dislocation damping and dislocation substructures is discussed.

Keywords: Ultrasonic Velocity, Dislocation Substructure, Stacking Fault Energy, Dislocation Damping

1. Introduction

The differences in the deformation behavior of metallic materials are generally known to be due to the differences in their stacking fault behaviors. The equilibrium separation distance of two partial dislocations varies inversely with the stacking fault energy (SFE). The SFE of an alloy strongly depends on the chemical composition. For a copper-based alloy, the SFE is affected by the electron/atom (e/a) ratio of the material. It is reported that with an e/a>1.1, the stacking fault energy usually decreases below 20 mJ/m^2 (Thornton et al., 1962). The movement of a partial dislocation is restricted to the plane of the faulted region. Also, different slip modes will exist with respect to the SFE. For a material with a high stacking fault energy, the partial dislocation separation is small (about 1*b* or less, *b* is the Burgers vector); therefore, little stress is necessary to recombine the partial dislocations. However, the separation of each partial dislocation is large (about 10-20*b*) in a low stacking fault energy material; therefore, the force necessary for recombination is large.

Different dislocation substructures will evolve due to plastic deformation and; moreover, the slip mode at the surface will be different (i.e. wavy slip in high SFE materials and planar slip in low SFE materials). For a wavy slip material, where cross slip easily takes place as a result of a high SFE, decomposition of the persistent slip bands (PSB) into the cellular bands will occur, resulting in a cell structure at high strain amplitude (El-Manhoun et al., 2003; Feltner and Laird, 1967; Kim et al., 2008). On the other hand, for a planar slip material, where it is difficult for cross slip to occur due to the low

Received: October 14, 2008, Revised: November 29, 2008, Accepted: December 3, 2008. * Engineering Science and Mechanics, Pennsylvania State University, 212 EES Building, State College, PA 16802, USA ** Department of Materials Science and Engineering, Seoul National University of Technology, Gongneungdong Seoul 139-743, Korea *** Department of Mechanical Engineering, Seoul National University of Technology, Gongneungdong Seoul 139-743, Korea † Corresponding Author: ikpark@snut.ac.kr

SFE, a planar array dislocation substructure will evolve (Kim et al., 2005; Lukas and Klesnil, 1973).

The type of dislocation substructures typical for the entire volume of specimens will depend very strongly on the strain amplitude, the stacking fault energy and, to a small extent, on the temperature. Feltner and Laird presented a simple schematic diagram relating the types of internal substructures (i.e. those typical for the whole volume) with these parameters (Feltner and Laird, 1968). Later, Lukas and Klesnil showed that a similar diagram, having a three regions with different dislocation substructure types, can be applied for both the internal and near surface substructures (Lukas and Klesnil, 1973). High stacking fault energy materials, when cycled in the low amplitude region, exhibit a vein or bundle structure. Whereas, the same materials cycled with high amplitudes exhibit a cell structure. In the low stacking fault energy materials the typical substructure is a planar array distribution of dislocations. Yaguchi et al. studied the fatigue damage evaluation in aluminum heat-transfer tubes by measuring the dislocation cell-wall thickness, and summarized the dislocation observation results at various stress amplitudes (Yaguchi et al., 2001). Under high stresses, basically, only the cell structure was observed; whereas, under low stresses, where the fatigue life was 10^7 times greater, only a vein or vein-like structure was observed. Under even lower stresses, only a simple increase in the dislocation density took place, and no clear dislocation structure developed. At medium stress amplitudes, where the fatigue life was between approximately 10^4 and 10^7 cycles, a mixture of cell, vein and possibly wall structures were observed.

Although the dislocation substructure of Al and Cu alloys subjected to plastic deformation have been analyzed by various groups using metallurgical method, to our knowledge, no studies of on the discrimination of dislocation substructures using nondestructive technique have been reported. The aim of this study is to investigate the influence of dislocation on ultrasonic velocity, and discriminate the dislocation substructures evolved from tensile deformation using ultrasonic velocity measurement.

2. Experimental Details

Our aim was to intentionally generated dislocation in specimens by applying plastic deformation and to take only the dislocation density and dislocation substructure as the main microstructural variable by minimizing the change in texture, which is one of the major factors affecting the ultrasonic velocity. For this purpose, the specimens were deformed with different tensile strains at room temperature. For the designed specimen, the microstructure was observed using a destructive method, and the ultrasonic velocity measured with a nondestructive method. In this study, Cu (78 mJ/m^2), Cu-35Zn (15 mJ/m^2, 8 mJ/m^2), 2.25Cr-1Mo steel (40-80 mJ/m^2), and AISI 316 ($\approx$20 mJ/m^2) were prepared, which are different SFE materials (Chattopadhyay, 2001; Dastur and Leslie, 1981; Kim, 2007; Plumtree and Abdel-Raouf, 2001; Rauch, 2004). The chemical compositions of the test materials are shown in Table 1. The test materials; Cu, Cu-35Zn, 2.25Cr-1Mo steel and AISI 316, were annealed at 450 ℃, 600 ℃, 950 ℃ and 1100 ℃, respectively. Initially, stress-strain curves for each test material were constructed by conducting tensile tests at room temperature. Based on the tensile test, specimens with different strains were prepared using the interrupt test.

In the direct contact method, where the ultrasonic waves are introduced into the test specimen through a contact medium, the experimental results are influenced by the thickness and viscosity of the couplant as well as the contact pressure. Also, ultrasonic pressure fluctuations in the near field make it hard to obtain a detailed measurement. Therefore, in this

Table 1 Chemical composition of test materials with different SFE (wt.%)

	C	Si	Mn	P	S	Ni	Cr	Mo	Pb	O2	Zn	Cu	Fe
Cu										<7.5ppm		Bal.	
Cu-35Zn									0.016		34.69	Bal.	0.017
2.25Cr-1Mo	0.138	0.14	0.46	0.01	0.004		2.27	0.97					Bal.
AISI 316	0.021	0.4	2.1	0.3	0.005	11.21	16.09	0.063					Bal.

work, the immersion test, a non-contact method, was employed to avoid this problem. During the immersion test, both the specimen and probe are immersed in water which acts as an effective energy transfer medium. For receiving and transmitting the ultrasonic waves, a pulser/ receiver (Panametric 5800) was used. For A/D conversion and data acquisition, a digital storage oscilloscope (Lecroy 9374M) was used. The sampling frequency of the oscilloscope was 5 GHz, with a resolution of 1 nsec in the time domain. Also, to remove the noise signal, a signal was obtained by averaging 1000 signals over time. A broad band piezoelectric transducer, with a central frequency of 9.6 MHz and diameter of 6.35 mm was used. The ultrasonic velocity was measured using the pulse echo method. For precise ultrasonic velocity measurements, all the samples were ground uniformly to a thickness of 10 mm, with the opposite faces planed parallel to within ±1 ㎛. The ultrasonic velocity was obtained with an accuracy of ±2 m/s. Also, the ultrasonic velocity was measured in the direction parallel to the tensile axis. All specimens were carefully electro polished in order to minimize the surface scattering and eliminate the deformed layer during sample preparation.

3. Results and Discussion

Fig. 1 shows the relative variation in the ultrasonic velocity for each material with respect to engineering strain. The ultrasonic velocity decreased with increasing strain. In Fig. 2, the Vicker's hardness change of these specimens is shown with respect to the change in strain. With an increase in the tensile strain, the Vicker's hardness also increased, with a larger change occurring during the initial stage. This is similar to work hardening under tensile deformation.

The variation in the ultrasonic velocity with tensile strain was different for each test specimen. The ultrasonic velocities of Cu and

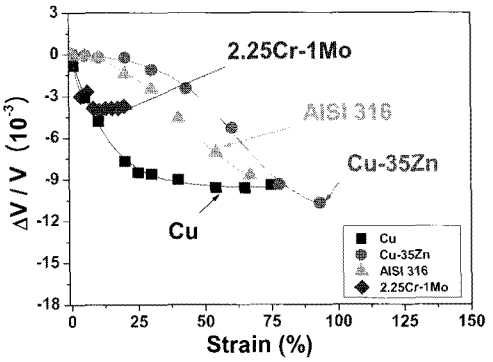

Fig. 1 Relative variation in longitudinal wave velocity at each material as a function of tensile strain

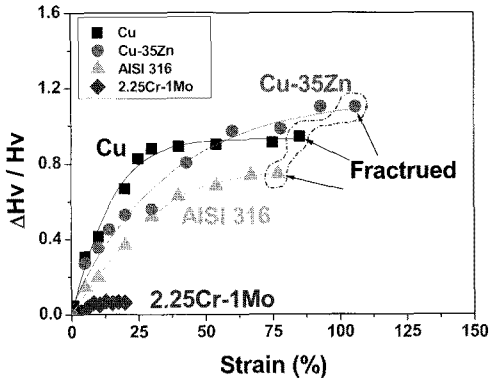

Fig. 2 Relative variation in Vicker's hardness at each material as a function of tensile strain

2.25Cr-1Mo steel, which are relatively high SFE materials, decreased rapidly during the initial stage, and then became saturated. However, the Cu-35Zn and AISI 316, which are low SFE materials, showed no plateau region.

This plateau phenomenon was also seen in the hardness test results, as shown in Fig. 2. From the view point of dislocation, the variation in the ultrasonic velocity was considered to show a close relationship to the dislocation density. During the initial stage, the dislocation density of these materials increased with increasing tensile strain deducing the work hardening, as did the flow stress and hardness. At the plateau region, the flow stress and hardness hardly increased, despite of the increase in strain, where the dislocation density is no longer increased through dynamic recovery. However, the hardness and flow stress of the low SFE materials uneventfully increased to the necking point and; thus, the dislocation density was thought to have increased during tensile deformation, and without any distinct dynamic recovery. Fig. 3 shows typical TEM micrographs for each fractured test specimen. The high SFE materials; Cu and 2.25Cr-1Mo steel; formed dislocation cell structures, but the low SFE materials; AISI 316 and Cu-35Zn, developed planar array dislocation substructures.

The effect of dislocation on ultrasonic velocity has been discussed by Granato and Lűcke (Granato and Lűcke, 1956). In their dislocation

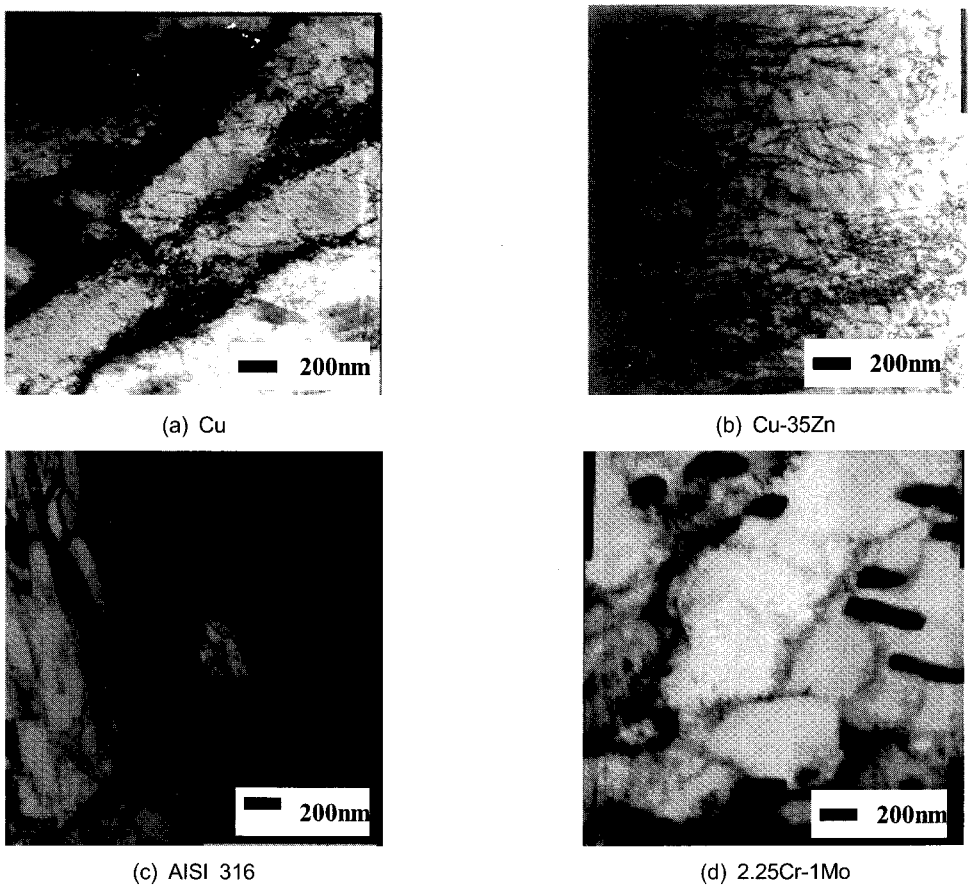

(a) Cu (b) Cu-35Zn

(c) AISI 316 (d) 2.25Cr-1Mo

Fig. 3 TEM micrographs of each fractured specimens showing different dislocation substructure: (a) well developed dislocation cell structure of pure Cu, (b) planar dislocation substructure of Cu-35Zn alloy, (c) planar substructure of AISI 316 in grain boundary, and (d) cell structure in 2.25Cr-1Mo steel and precipitates

damping model, a dislocation is regarded as a vibrating string between pinning points. Dislocation line segment vibrates under the influence of ultrasonic stress field with a phase lag because of lattice viscosity, and also the acoustic energy is absorbed. This inelastic mechanism also lowers the ultrasonic velocities. The dislocation lines are pinned by point defects, vacancies and interstitials. The pinning points acted as nodes of the dislocation segment vibrations. Assuming strain amplitude independent damping, the velocity change ($\triangle V = V_0 - V$, V_0 is the velocity in an ideal solid, in which dislocations are absent) is given in a low frequency ranges by this following equation:

$$\triangle V / V_0 = -\left(\frac{4Gb^2}{\pi^4 C}\right)\Lambda L^2$$

where, G is the shear modulus, b the Burgers vector magnitude, Λ the dislocation density, L is dislocation-loop length, and C denotes the dislocation-line tension.

According to the dislocation damping model, the equation indicates that the increase of the dislocation density and loop length leads to the decrease of the ultrasonic velocity. That is, the velocity is proportional to Λ and the second power of the segment length L of the dislocations that are able to move with the ultrasonic wave. However, note that this above equation is not applied to all the dislocation and is aimed at dislocation that vibrates with the ultrasonic stress field. Therefore, these movable dislocations (i.e. effective dislocation) make away with the dislocations tangled and piled up at grain boundaries or subgrain boundaries. In addition, dislocation is a typical lattice defect which distorts the lattice of solid, thereby generates the strain field around dislocations (Kim et al., 2008). The strain field in the vicinity of dislocation may disturb the ultrasonic wave during propagation in the solid media resulting in decrease of the ultrasonic wave velocity. Moreover, the magnitude of distortion is proportional to the dislocation density. From the above reasons, we can understand that the ultrasonic velocity change observed in this study is dominantly dependent on the effective dislocation density and pinning point separation.

Although initial variation in ultrasonic velocity could be well understood with respect to dislocation damping model, the saturation of ultrasonic velocity in high SFE materials and monotonic change for low SFE materials could not be explained clearly. High SFE materials, Cu and 2.25Cr-1Mo steel, developed cell dislocation structure, where the effective dislocations in the interior of the cell subgrains could not be easily observed due to piled up at the subgrain boundaries. But low SFE materials, Cu-35Zn and AISI 316, evolved planar dislocation structure, where the band width narrowed with tensile deformation without any dynamic recovery. Furthermore, these edge dislocations in band structure could easily move on the same slip plane, between bands, vibrate with respect to ultrasonic wave. This mechanism is not clear, and it is a subject for future investigation.

4. Conclusion

The ultrasonic velocity kept decreasing with increasing strain in all the test materials. Especially, the ultrasonic velocity became saturated with plastic strain in both the Cu and 2.25Cr-1Mo steel. However, in the Cu-35Zn and AISI 316, no plateau phenomenon was observed. This phenomenon is thought to be closely related with the SFE of the test materials. The high SFE materials (i.e. Cu and 2.25Cr-1Mo steel) showed a saturation state, indicating dynamic recovery. The ultrasonic velocity decreases with increases in the dislocation density. Also, the dislocation formed due to tensile deformation causes lattice distortion, which decreases the ultrasonic velocity. Consequently, the ultrasonic velocity is strongly influenced by the dislocation structure, and we can successfully discriminate the dislocation substructures with nondestructive technique.

Acknowledgments

This work was supported by the Korea Research Foundation Grant funded by the Korean Government (MOEHRD) (KRF-2007-375-D00003)

References

Chattopadhyay, R. (2001) Surface Wear: Analysis, Treatment, and Prevention, *ASM International,* pp. 25-38

Dastur, Y. N. and Leslie, W. C. (1981) Mechanism of Work Hardening in Hadfield Manganese Steel, *Metallurgical Transactions A*, Vol. 12, pp. 749-759

El-Madhoun, Y., Mohamed, A. and Bassim, M. N. (2003) Cyclic Stress-Strain Response and Dislocation Structures in Polycrystalline Aluminum, *Materials Science and Engineering A*, Vol. 359, pp. 220-227

Feltner, C. E. and Laird, C. (1967) Cyclic Stress-Strain Response of F.C.C. Metals and Alloys-II Dislocation Structures and Mechanism, *Acta Metallurgica*, Vol. 15, pp. 1633-1653

Feltner, C. E. and Laird, C. (1968) Factors Influencing Dislocation Structures in Fatigued Metals, Transactions of the American Institute of Mining, *Metallurgical and Petroleum Engineers*, Vol. 242, No. 7, pp. 1253-1257

Granato, A. and Lűcke, K. (1956) Theory of Dislocation Damping due to Dislocations, *Journal of Applied Physics,* Vol. 27, No. 6, pp. 583-593

Kim, C. S., Kim, Y. H. and Kim, I. H. (2005) Ultrasonic Linear and Nonlinear Parameters in Cyclically Deformed Cu and Cu-35Zn Alloy, *Key Engineering Materials*, Vol. 297-300, No. 3, pp. 2134-2139

Kim, C. S. (2007) Nondestructive Assessment of Microstructural Change by Fatigue and Creep, Ph. D. Thesis, Korea University, Korea, pp. 46-77

Kim, C. S., Park, I. K., Jhang, K. Y. and Kim, N. Y. (2008) Experimental Characterization of Cyclic Deformation in Copper Using Ultrasonic Nonlinearity, *Journal of the Korean Society for Nondestructive Testing,* Vol. 28, No. 3, pp. 285-291

Kim, C. S., Kwun, S. I. and Park, I. K. (2008) Characterization of Creep-Fatigue in Ferritic 9Cr-1Mo-V-Nb Steel Using Ultrasonic Velocity, *Journal of Nuclear Materials*, Vol. 377, pp. 496-500

Lukas, P. and Klesnil, M. (1973) Cyclic Stress-Strain Response and Fatigue Life of Metals in Low Amplitude Region, *Materials Science and Engineering A*, Vol. 11, pp. 345-356

Plumtree, A. and Abdel-Raouf, H. A. (2001) Cyclic Stress–Strain Response and Substructure, *International Journal of Fatigue*, Vol. 23, pp. 799-805

Rauch, E. F. (2004) Effects of Metal Characteristics and Experimental Conditions on Dislocation Self-Organization, *Revue de Metallurgie. Cahiers D'Informations Techniques*, Vol. 101, No. 2, pp. 1007-1019

Thornton, P. R., Mitchell, T. E. and Hirsch, P. B. (1962) The Dependence of Cross-Slip on Stacking-Fault Energy in Face-Centred Cubic Metals and Alloys, *Philosophical Magazine*, Vol. 7, No. 80, pp. 1349-1369

Yaguchi, H. (2001) Fatigue-Damage Evaluation in Aluminum Heat-Transfer Tubes by Measuring Dislocation Cell-Wall Thickness, *Materials Science and Engineering A*, Vol. 315, pp. 189-194